

## Abstract

In case of seismic design the deformability of the soil should be considered, which can be performed in several ways. Most of the methods do not take into account the finite dimensions of the soil, which results significantly different behavior than the spring-dashpot systems. For an infinite medium, which is used in many cases, there are no eigenmodes, however in practical applications the soft soil is always bounded by rocks. For these cases the soil has eigenmodes and the resonance may influence considerably the response of the system. This question was investigated numerically by FE calculations, and it was found that in certain cases the resonance, which is neglected in the common design process, may significantly enhance the earthquake loads. In this paper this phenomenon is investigated and the parameter range is defined when this effect must be taken into account.

## Keywords

soil-structure interaction, resonance, impedance, direct approach

## 1 Introduction

In case of static design fixed foundation can be assumed, however in case of earthquake resistant design the effect of the soil must be taken into account. The soil influences the response of the structure in different ways. The seismic event in the absence of the structure causes a free-field motion in the soil, which is different from the case when the structure is present (kinematic and inertial interaction [1]). In case of infinite soil layer the phenomenon of radiation damping occurs, due to the fact that the strain and kinetic energies are dissipated through wave propagation towards infinity [2]. The dynamic loading of a finite soil layer can cause resonance, which may significantly change the response of the structure. Neglecting these different effects may result in significant errors in the analysis.

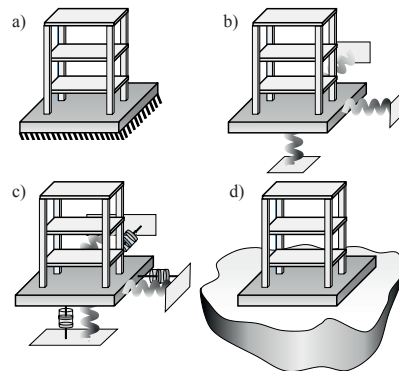


Fig. 1 Levels of modeling the effect of soil: a) fixed support, b) elastic support, c) substructure approach, d) direct approach

Soil-structure interaction can be taken into account in different ways (Fig. 1). The deformability of the soil can be considered by using elastic support (Fig. 1b). There are several formulas in the literature for the stiffness characteristics of an infinite half-space [3], and the stiffness of a finite soil layer can be calculated by static finite element method. A more sophisticated method is the substructure approach [1], where the response of the structure is calculated by superposition. First the excitation on the free soil surface is determined from the excitation on the bed rock, then the impedance of the soil-structure system is calculated. The soil-structure

<sup>1</sup> Department of Structural Engineering  
 Faculty of Civil Engineering,  
 Budapest University of Technology and Economics  
 H-1111 Budapest, Műegyetem rkp. 3, Hungary

\* Corresponding author, email: [pap.zsuzsa@epito.bme.hu](mailto:pap.zsuzsa@epito.bme.hu)

interaction is obtained by superposition; and hence the method is (directly) applicable for linear systems only. In this case the radiation damping is represented by dashpot elements (Fig. 1c). Finally, the most accurate approach is the direct method (Fig. 1d), where the soil and the structure are modeled together. In this case nonlinearities can also be considered, however it requires significant computational effort.

The simplified spring-dashpot models are derived from the impedance function of soil with a weightless foundation [1], where the foundation is excited by a harmonic force (Fig. 2). The ratio of this force and the displacement of the foundation is the impedance function, which depends on the excitation frequency. This function consists of an amplitude and a phase angle (the shift of the force and displacement). These can be interpreted as a spring stiffness and a damping value, but these parameters depend on the excitation frequency. As a simplified method, these functions are often approximated by constant values (usually the initial values) [3].

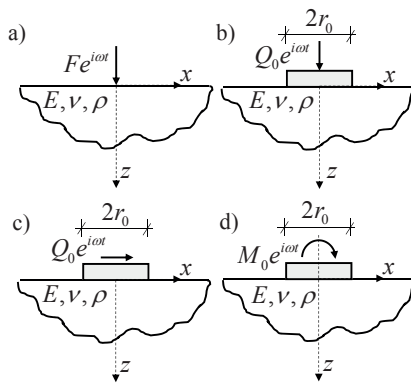


**Fig. 2** a) Half-space under concentrated harmonic force, b) half-space with foundation loaded by vertical harmonic force, c) half-space with foundation loaded by horizontal harmonic force, d) half-space with foundation loaded by harmonic rocking moment

( $F, Q_0$  is the amplitude of the harmonic force,  $M_0$  is the amplitude of the harmonic rocking excitation,  $\omega$  is the frequency of excitation,  $r_0$  is the radius of foundation,  $E$  is the elastic modulus,  $\nu$  is the Poisson's ratio and  $\rho$  is the density of soil)

The impedance function of the soil half-space for vertical translational force was investigated by Lamb [4]. He gave a complex analytical function as a solution. Reissner [5] analyzed a soil half-space with a circular foundation, and also gave a complex function as the impedance, he denoted the real part by  $F_1$  and the complex part by  $F_2$ :

$$\frac{Q(t)}{u(t)} = Gr_0 [F_1 + iF_2], \quad (1)$$

where  $Q$  is the harmonic force,  $u$  is the vertical displacement,  $G$  is the shear modulus of the soil and  $r_0$  is the radius of the foundation.

Sung [6] investigated different stress distributions under the foundation. Hsieh [7] derived frequency dependent spring stiffness and damping values from the complex impedance

functions. These frequency dependent stiffness and damping values are approximated by constant values by Lysmer and Richart [8] for vertical excitation and by Bycroft [9] for horizontal and rocking motion. Shah [10] analyzed both circular and strip foundations for translational and rocking motions. Approximate values for spring stiffnesses and damping values are summarized in [11] and [12] for different motions, foundation shapes for both half-space and finite soil layers.

The cone model [13], [2] also gives constant spring stiffnesses and damping coefficients according to the analytical solution of a semi-infinite cone under harmonic excitation. Barros and Luco [14] and J. P. Wolf [15] examined systems consisting of several spring stiffnesses, dashpots and masses by determining the different parameters by the least square method.

Most of the methods do not take into account the finite dimensions of the soil, which results significantly different behavior than the spring-dashpot systems. For an infinite medium, which is used in many cases, there are no eigenmodes, however in practical applications the soft soil is always bounded by rocks. For these cases the soil has eigenmodes and the resonance may influence considerably the response of the system.

## 2 Problem statement

In case of practical earthquake resistant design the applicability of frequency dependent impedance function is very limited, because its complexity. Rather, engineers are applying constant spring stiffnesses and damping values according to one of the formulas in the literature [11] which are based on the impedance function of a soil half-space, or to calculate a constant spring stiffness by static finite element analysis. None of these are taking into account the possible resonance which may occur in case of the dynamic loading of a finite soil layer.

The goal of this paper is to investigate the significance of the effect of resonance, and to determine the maximum error, which can occur neglecting it in the design process.

## 3 Approach

A finite soil layer with a rigid foundation (Fig. 3a and b) and the simplified (spring-dashpot) models (Fig. 3c) are analyzed numerically to determine the effect the resonance. The analyses are limited to horizontal and rocking motion of the foundation. The numerical analysis was performed by the ANSYS computer code. Harmonic and time-history analyses were executed, and different signals were investigated (harmonic excitation, real and artificial earthquake records).

## 4 Modelling of SSI

As it was stated in the Introduction the modelling of soil-structure interaction can be achieved by different methods. In the following sections the direct approach and different simplified models are discussed.

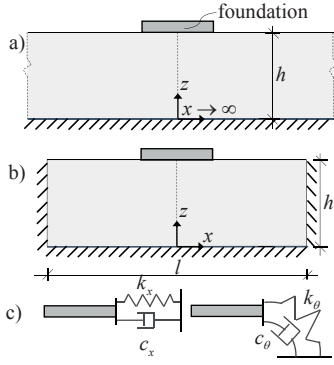


**Fig. 3** a) Finite soil layer with thickness  $h$  and rigid foundation, b) finite soil layer with side-boundaries, c) simplified model with constant spring stiffness and dashpot element

#### 4.1 Direct approach

In the direct approach the structure and the soil have to be modelled together (Fig. 1d) and analyzed in a single step with a numerical method such as the finite element method. 2D models were built to analyze soil layers with strip foundations with the aid of the 14.5 release of ANSYS Mechanical APDL.

#### 4.2 Simplified models

In the literature there are several solutions for the impedance functions of a half space with circular or strip foundation [9], [10]. As it was mentioned in the Introduction, the impedance can be given by a complex function. In case of the inverse impedance ( $Z = u(t)/Q(t) = 1/Gr_0[f_1 + f_2]$ )  $f_1$  represents the real part and  $f_2$  the complex part of the function. These can be also given as an amplitude and a phase angle:

$$Z_0 = \frac{1}{Gr_0} \sqrt{f_1^2 + f_2^2}, \quad \varphi = \tan^{-1}(f_1 + f_2). \quad (2)$$

Furthermore, the function can also be given as frequency dependent spring stiffness and damping [7]:

$$k(\omega) = Gr_0 \frac{f_1}{f_1^2 + f_2^2}, \quad c(\omega) = \frac{Gr_0}{\omega} \frac{-f_2}{f_1^2 + f_2^2}. \quad (3)$$

In the simplified model, these frequency dependent functions are approximated by constant values (Fig. 4).

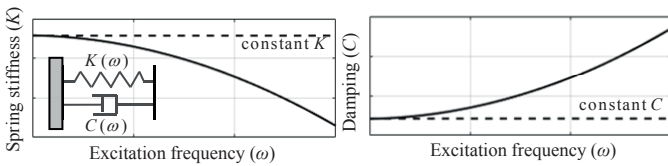


**Fig. 4** Approximation of the spring stiffness and damping with constant values [16]

The constant spring stiffness and damping values for strip foundation in case of horizontal excitation are [11]:

$$k_x = \frac{2.24}{2-\nu} G, \quad c_x = 2r_0 \sqrt{\rho G}, \quad (4)$$

where  $G$  is the shear modulus,  $\nu$  is the Poisson's ratio of the soil and  $r_0$  is the half width of the strip foundation.

The approximate constant spring stiffness and damping values for rocking excitation [11]:

$$k_\theta = \frac{8Gr_0^2}{2(1-\nu)} \left[ 1 + \left( \frac{\ln(3-4\nu)}{\pi} \right)^2 \right], \quad c_\theta = \frac{3.4\sqrt{G\rho}}{\pi(1-\nu)} I_0, \quad (5)$$

where  $I_0$  is the moment of inertia of the structure.

### 5 Effect of resonance of the finite soil layer

In this section the horizontal and rocking motion of a finite soil layer (Fig. 3a) is investigated. In case of soil-structure interaction the impedance function is the ratio of the harmonic force excitation of the weightless foundation and the steady-state solution of the displacement for different excitation frequencies. Therefore, the peaks of the function show the resonant points, i.e. the eigenfrequencies of the soil layer. To determine the impedance function of a finite soil layer, harmonic analysis is performed. For this the mode superposition method of the harmonic analysis in ANSYS is used. The frequency step is set to  $10^{-4}$  1/s and the solution is clustered about the system's natural frequency to accurately tracing the response curve. The material damping is  $\zeta = 0.05$  in every analysis.

#### 5.1 Harmonic analysis for horizontal motion

The  $n^{\text{th}}$  resonant frequency of a free soil layer can be approximated by the  $n^{\text{th}}$  resonant frequency of a sheared beam [17]:

$$f_n = \frac{c_s}{2h} \left( n - \frac{1}{2} \right), \quad n = 1, 2, 3 \dots \quad (6)$$

where  $c_s$  is the shear wave velocity in the soil,  $h$  is the thickness of the soil layer. The shear wave velocity of the soil represents the stiffness of the soil ( $G = \rho c_s^2$ ) [18].

The natural frequency of a soil layer with a weightless foundation will be different, since this formula is based on a 1D model, but in the case of a rigid (strip) foundation the displacements will be 2D and in case of a circular foundation 3D.

In Fig. 5, Fig. 6 and Fig. 7 the inverse of the impedance functions of soil layers with different parameters are presented. The inverse of the impedance functions calculated for a finite soil layer (Fig. 3a) by FE are given on two diagrams ( $Z = u(t)/Q(t)$ ), the first one shows the amplitude, the second one shows the phase angle, which is the shift between the force and displacement. (This shift represents the energy dissipation of the system, e.g. when only a mass-dashpot system is considered, the phase angle in the impedance function is  $90^\circ$ , while for zero shift the energy dissipation is zero.)

Fig. 5 shows the impedance function for different soil layer thicknesses ( $h$ ). As it can be seen the bigger the value of  $h$  is, the smaller the first natural frequency is (as in Eq. (6)). This means that the effect of the resonance for the amplitude of the displacement will be smaller for thicker soil layers. The curves are overlapping with each other, if on the horizontal axis the

frequency is multiplied with the thickness of the soil layer ( $h$ ) and the amplitude is normalized with the static stiffness. The normalized diagram is showed for different  $r_0/h$  values in Fig. 9.

$$Z_0 = \frac{1}{k_x + \frac{c_x^2 \omega^2}{k_x^2}}, \quad \varphi = \arctan\left(-\frac{c_x \omega}{k_x}\right). \quad (7)$$

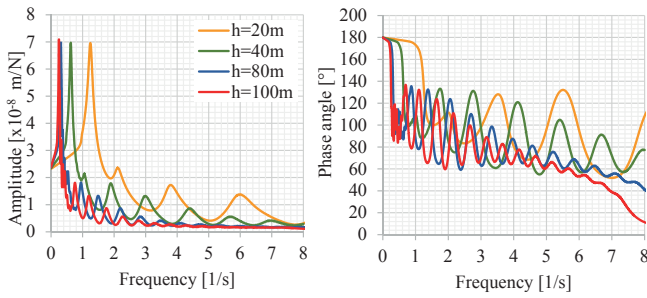


**Fig. 5** Horizontal inverse impedance function of soil layer for different soil thicknesses ( $h$ )

( $c_s = 100$  m/s,  $\nu = 0.3$ ,  $\rho = 1800$  kg/m<sup>3</sup>,  $\zeta = 0.05$ ,  $r_0 = 5$  m)

In Fig. 6 the effect of the shear wave velocity (i.e. stiffness of the soil) is shown. The diagram of the amplitude shows that in case of soft soils (small  $c_s$ ) the effect of the resonance is much more dominant than in case of stiffer soils. Similarly to the previous case, the curves are overlapping, if the horizontal axis is divided by the shear wave velocity ( $c_s$ ) and the vertical axis is normalized with the initial value of the amplitude ( $1/k_{\text{static}}$ ). The normalized diagram is given in Fig. 9.

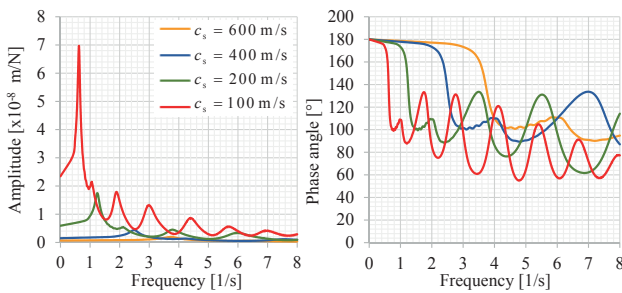


**Fig. 6** Horizontal inverse impedance function of soil layer for different shear wave velocities ( $c_s$ )

( $h = 40$  m,  $\nu = 0.3$ ,  $\rho = 1800$  kg/m<sup>3</sup>,  $\zeta = 0.05$ ,  $r_0 = 5$  m)

Fig. 7 shows the impedance for different Poisson ratios. In this case the curves for the amplitude and phase angle are almost on the top of each other, for smaller  $\nu$ , the amplitude is slightly bigger.

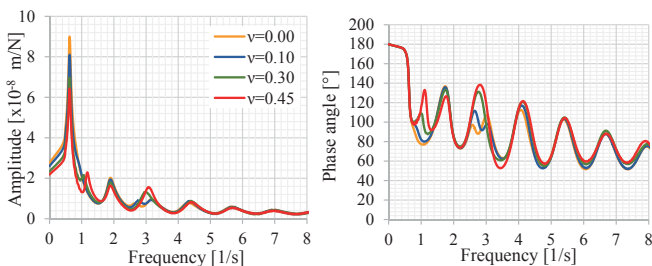


**Fig. 7** Horizontal inverse impedance function of soil layer for different Poisson ratios ( $\nu$ )

( $c_s = 100$  m/s,  $h = 40$  m,  $\rho = 1800$  kg/m<sup>3</sup>,  $\zeta = 0.05$ ,  $r_0 = 5$  m)

The inverse impedance function of a spring-dashpot system (in case of unit force) as an amplitude and phase angle are given in Fig. 8:

If we compare the functions in Fig. 5, Fig. 6 and Fig. 7 to the function in Fig. 8, the difference between the amplitude is extremely high, and the phase angle is also different in this frequency range.

A common method in practical earthquake resistant design is to consider the effect of the soil by calculating a constant spring stiffness ( $k_{\text{static}}$ ) with the aid of a static finite element calculation. In that case the amplitude of the inverse impedance function is  $1/k_{\text{static}}$  ( $2.32 \cdot 10^{-8}$  m/N for the same parameters as in Fig. 8).

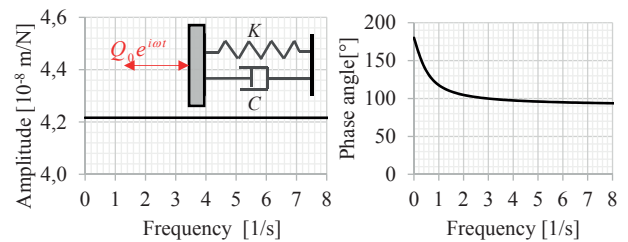


**Fig. 8** Horizontal inverse impedance function of spring-dashpot system calculated by Eq. (4) and Eq. (7) ( $c_s = 100$  m/s,  $\rho = 1800$  kg/m<sup>3</sup>,  $r_0 = 5$  m)

The inverse impedance function of a finite soil layer with strip foundation (Fig. 3a) is summarized in Fig. 9. The amplitude is normalized with the initial (static) value of the amplitude ( $1/k_{\text{static}}$ ), and it is given in the function of a dimensionless frequency parameter ( $fh/c_s$ ) for different  $r_0/h$  ratios, where  $r_0$  is the half width of the foundation.

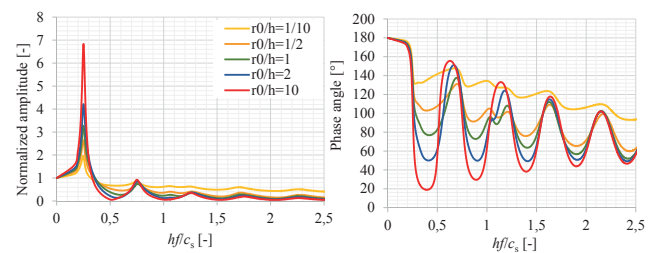


**Fig. 9** Normalized inverse impedance function for horizontal motion and for different  $r_0/h$  ratios

Fig. 10 shows the ratio of the inverse horizontal impedance function for different  $r_0/h$  ratios, when the function is bigger than 1 the approximation is not conservative, when it is smaller than 1 it is conservative. It can be seen that  $r_0/h = 10$  the amplitude in case of the soil layer can be 7 times bigger than the amplitude of the spring-dashpot model, because of the first natural frequency of the soil layer, while for small  $r_0/h$  value the ratio of the amplitudes is around 2. The right diagram of Fig. 10 shows the ratios of the phase angle. In case of small  $r_0/h = 1/10$  the ratio of the phase angles is around 1, while for bigger  $r_0/h$  ratios the phase angle of the soil layer can be 5 times smaller than in case of the spring-dashpot model.

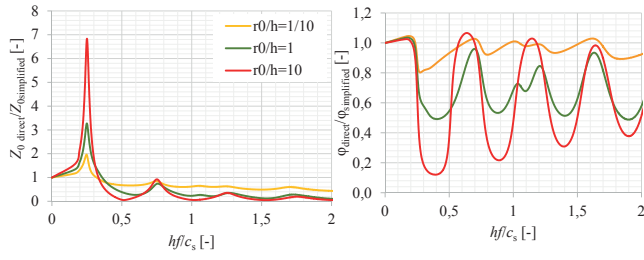
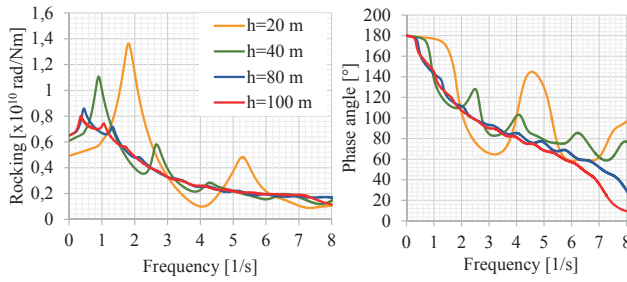


**Fig. 10** Ratio of the inverse, horizontal impedance function of the soil layer (Fig. 3a) and the simplified spring-dashpot model (Fig. 3c) (deviation from unity shows the error of the simplified model)

## 5.2 Harmonic analysis for rocking motion

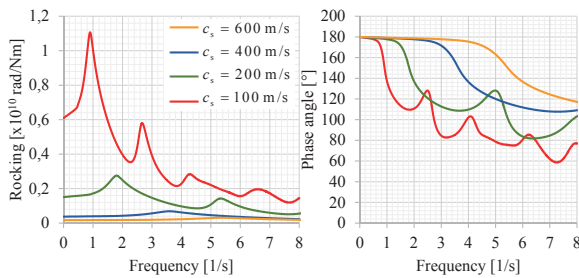
For rocking excitation similar inverse impedance functions can be calculated by FE for a finite soil layer (Fig. 3a). The effect of the different soil parameters are shown in Fig. 11 and Fig. 12.

Fig. 11 shows the amplitude and phase angle of the rocking inverse impedance function for different soil layer thicknesses. It can be observed, that in case of rocking motion not only the value of the natural frequencies are different in case of the different  $h$  values, but the amplitude is also changing. For larger soil layer thicknesses the peaks are disappearing.



**Fig. 11** Rocking inverse impedance function of soil layer for different soil thicknesses ( $h$ ) ( $c_s = 100$  m/s,  $\nu = 0.3$ ,  $\rho = 1800$  kg/m<sup>3</sup>,  $\zeta = 0.05$ ,  $r_0 = 20$  m)

The effect of the soil stiffness to the impedance function can be observed in Fig. 12. Similarly to the horizontal motion, the effect of resonance is much more significant in case of soft soils. For stiffer soils ( $c_s = 600$  m/s) the peaks are smaller in both the amplitude and phase angle curves.



**Fig. 12** Rocking inverse impedance function of soil layer for different shear wave velocities ( $c_s$ ) ( $h = 40$  m,  $\nu = 0.3$ ,  $\rho = 1800$  kg/m<sup>3</sup>,  $\zeta = 0.05$ ,  $r_0 = 20$  m)

Similarly to the horizontal case, the curves of Fig. 11 and Fig. 12 are overlapping when the horizontal axis is multiplied by the thickness of the soil layer ( $h$ ), divided by the shear wave velocity ( $c_s$ ) and the vertical axis is normalized by the static stiffness. In this case one curve belongs to all of the  $h$  and

$c_s$  values, but different curves belong to different  $r_0/h$  ratios (because this normalization does not include the effect of the width of the foundation). The normalized diagrams are shown in Fig. 13. For high  $r_0/h$  ratios the peaks are significant, while for small  $r_0/h$  ratios the peaks are disappearing.

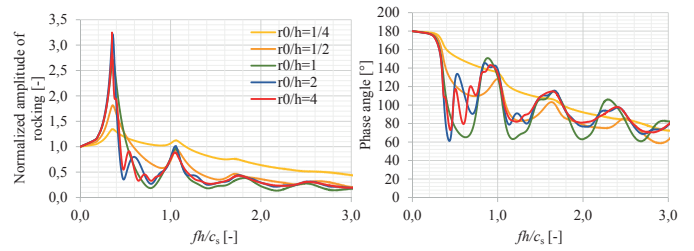


**Fig. 13** Normalized inverse impedance function for rocking motion and for different  $r_0/h$  ratios

To evaluate the difference between the rocking of a weightless strip foundation on a soil layer (Fig. 3a) and the simplified spring dashpot model (Fig. 3c), the ratios of the amplitude and phase angle of the rocking inverse impedances are given in Fig. 14. The ratios show that for big  $r_0/h$  ratio the rocking in case of the soil layer can be 3 times bigger than in case of the spring-dashpot model. For small  $r_0/h$  values the ratio of the amplitudes and phase angle of the two models are close to one, which means the simplified model gives a good approximation.

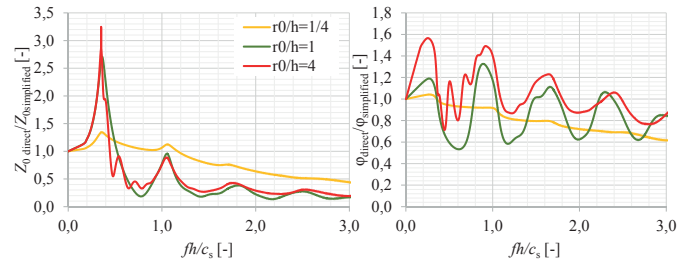


**Fig. 14** Ratio of the inverse, rocking impedance function of the soil layer (Fig. 3a) and the simplified spring-dashpot model (Fig. 3c) (deviation from unity shows the error of the simplified model)

## 6 Effect of the eigenfrequency of the soil-structure system

The effect of the resonance of the soil-structure system is also investigated. A rigid structure with mass  $M$  on a finite soil layer is considered. First harmonic analyses are performed, then the horizontal displacement of the foundation is calculated from base excitation (Fig. 15). The base excitation is  $u_g(t)$ , the horizontal displacement of the structure is  $u_{direct}(t)$  in case of the analysis of the finite soil layer (Fig. 15a) and  $u_{simplified}(t)$  for the simplified model (Fig. 15b).

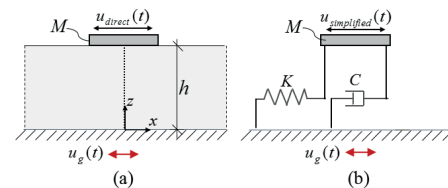


**Fig. 15** (a) Finite soil layer with thickness of  $h$  and rigid foundation with mass  $M$ , (b) Simplified model

## 6.1 Harmonic analysis for horizontal motion

First the two models (Fig. 15) for trigonometrical excitation are analyzed. Fig. 16 shows the difference between the horizontal displacement of the direct and simplified model and also for the case, when the spring stiffness is calculated by static FEM.

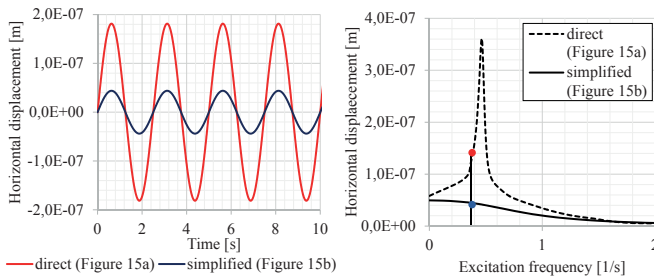


**Fig. 16** Horizontal displacement of the foundation for harmonic excitation ( $c_s = 100 \text{ m/s}$ ,  $\rho = 1800 \text{ kg/m}^3$ ,  $r_0 = 5 \text{ m}$ ,  $h = 40 \text{ m}$ ,  $M = 106 \text{ kg}$ ,  $\zeta = 0.05$ )

The left diagram of Fig. 16 shows the steady-state solution for  $f = 0.4 \text{ Hz}$  sine excitation, as it can be seen the maximum horizontal displacement of the direct model 5 times bigger than the displacement in case of the simplified model. The right diagram of Fig. 16 shows the amplitude for different frequencies, the difference between the models can be even higher for the frequencies close to the resonant point. The resonant frequency of the two models are also different, in this case  $f_0 = 0.46 \text{ Hz}$  for the direct model,  $f_0 = 0.71 \text{ Hz}$  for the simplified model.

## 6.2 Time-history analysis for earthquake record

To determine the effect of the resonance in the design process a soil layer with a rigid strip foundation and the simplified model is analyzed for earthquake excitation. To investigate the effect of resonance the parameters are chosen in such a way that the dominant frequency of the record is close to the soil-structure system's first natural frequency. The natural frequency of the simplified model is different (as it is shown in Section 6.1), therefore in this way the maximum of the possible error is presented.

In order to be able to compare the methods with each other artificial records are used, the accelerograms are generated from Eurocode response spectra. To calculate the horizontal displacement of the structure resting on a soft soil layer the bedrock under the soil is excited, and a record generated for curve A of EC 8 [19] is used. Fig. 17a shows the difference between the horizontal displacement of the structure resting on a finite soil layer (Fig. 15a) and the simplified model (Fig. 15b) for the artificial earthquake excitation generated for curve A. The horizontal displacement of the structure resting on a soil layer is 20 times larger than the horizontal displacement of the simplified model.

Note however that the common design process in case of the simplified modeling is to use the curve of the analyzed

soil type (in this case curve D [19]), to consider the amplification of the soil layer. In Fig. 17b the artificial record generated for curve A is used for the structure resting on a soil layer, while the record generated for curve D is used for the simplified model. In this case the horizontal displacement of the structure on a soil layer is 10 times higher than the horizontal displacement of the simplified model.

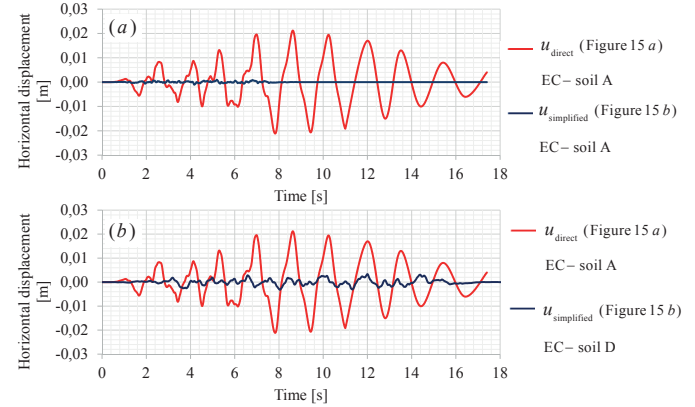


**Fig. 17** Horizontal displacement of the foundation for earthquake excitation a)  $u_{\text{simplified}}$  is calculated by an artificial earthquake generated for EC curve A, b)  $u_{\text{simplified}}$  is calculated by an artificial earthquake generated for EC curve D ( $c_s = 100 \text{ m/s}$ ,  $\rho = 1800 \text{ kg/m}^3$ ,  $r_0 = 20 \text{ m}$ ,  $h = 40 \text{ m}$ ,  $M = 105 \text{ kg}$ ,  $\zeta = 0.05$ )

## 6.3 Significance of the resonance

As it is shown in Sections 6.1 and 6.2 significant error can be made by using the simplified model, when the dominant frequency of the earthquake is close to the first eigenfrequency of the soil-structure system. The frequency content of typical earthquakes (analyzing the 44 far-field record of [20]) is in the range of  $0.45 < f < 2.82 \text{ 1/s}$ . Fig. 18 shows the resonance-sensitive zones according to the dominant frequency content of the analyzed records of the  $h$  and  $c_s$  parameters of the soil for different masses ( $M$ ). It can be observed that in case of bigger masses the softer soils are not affected.

## 7 Effect of finite length of soil layer

In the previous sections the effect of the resonance of a soil layer with finite thickness, and infinite horizontal dimensions is investigated. In reality there also may be vertical boundaries in the soil, e.g. there can be stiffer soil layers near the softer one.

### 7.1 Derivation of the natural frequency

To determine the natural frequency of a soil layer with the thickness  $h$  and length  $l$  (Fig. 19) the Rayleigh-Ritz method is used. The horizontal displacement is assumed in the following form:

$$u_x(x, z, t) = \bar{u}(x)A \sin\left(\frac{1}{2} \frac{\pi z}{h}\right) \{a_r \cos(\omega_0 t) + b_r \sin(\omega_0 t)\}, \quad (8)$$

where  $\bar{u}(x)$  is the displacement function in the  $x$  direction,  $h$  is the thickness of the soil layer,  $\omega_0$  is the natural circular frequency of the layer,  $A$ ,  $a_r$  and  $b_r$  are constants.

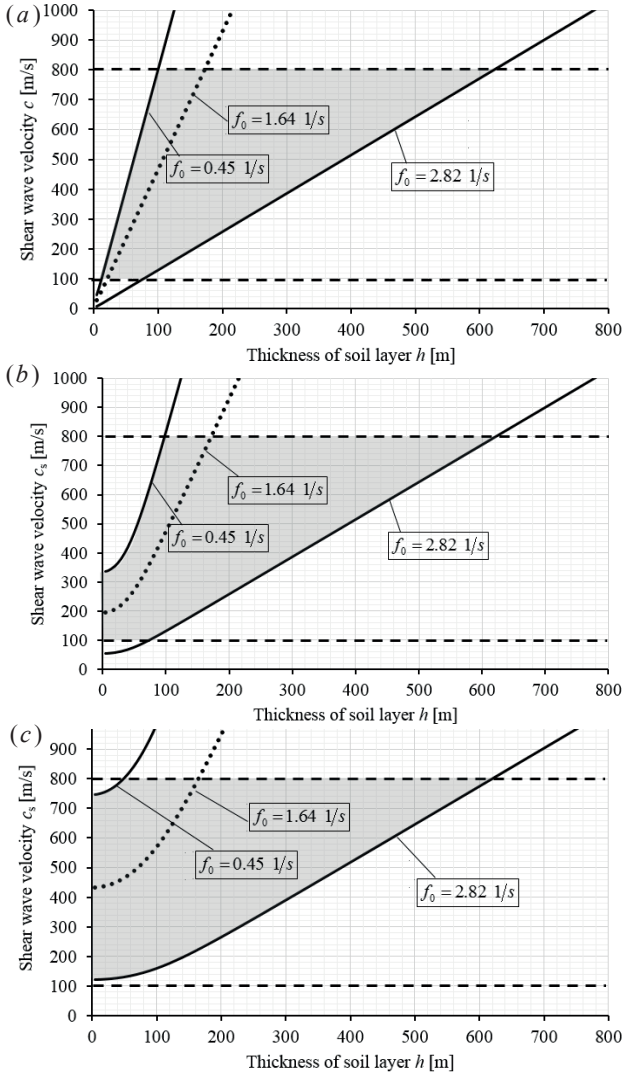


**Fig. 18** Parameter range ( $c_s$  and  $h$ ), where the natural frequency of the system is in the range of the dominant frequency of earthquakes, a)  $M = 10t$ , b)  $M = 1000t$ , c)  $M = 5000t$

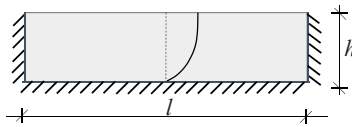


**Fig. 19** Soil layer and the assumed shape of horizontal displacement with thickness  $h$ , length  $l$

To obtain the natural frequency the kinetic ( $T$ ) and potential energy ( $U$ ) should be calculated. Fig. 7 shows that the effect of Poisson's ratio on the natural frequency is negligible, therefore in the derivation  $\nu = 0$  is assumed. The kinetic and the potential energy can be calculated from Eq. (8) in a straightforward manner:

$$T(\bar{u}(x)) = \frac{\rho h}{4} \omega_0^2 \int_x \bar{u}^2(x) dx, \quad (9)$$

$$U(\bar{u}(x)) = \frac{Eh}{4} \int_x \frac{d\bar{u}^2(x)}{dx} dx + \frac{E\pi^2}{32h} \int_x \bar{u}^2(x) dx, \quad (10)$$

where  $E$  is the elastic modulus,  $h$  is the thickness and  $\rho$  is the density of the soil layer.

The total mechanical energy (sum of kinetic and potential energy) is constant during free vibration. When the kinetic energy is maximal, the potential energy is zero, and vice versa. Therefore, the maximum potential and kinetic energy are equal to each other:

$$T_1^{\max} = U_1^{\max} \Rightarrow \frac{\rho A^2 h l}{8} \omega_0^2 = \frac{EA^2 h \pi^2}{8l} + \frac{EA^2 \pi^2 l}{16h}, \quad (11)$$

where  $l$  is the length of the soil layer Fig. 19.

The natural circular frequency of the soil layer with finite thickness and length is obtained from Eq. (11):

$$\omega_0 = \sqrt{\frac{E\pi^2}{\rho} \left( \frac{1}{8h^2} + \frac{1}{l^2} \right)}. \quad (12)$$

It can be observed that when the length is infinite Eq. (12) is identical to Eq. (6). Fig. 20 shows the change in the natural frequency as a function of the length-thickness ratio ( $l/h$ ) of the soil layer.

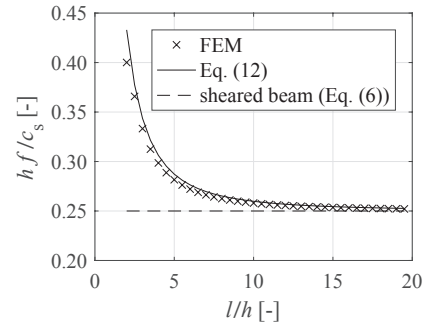


**Fig. 20** Natural frequency of soil layer with thickness  $h$ , length  $l$  and shear wave velocity  $c_s$

Fig. 21 shows the inverse impedance function for soil layers with finite length and thickness for two  $l/h$  ratios ( $l/h = 2$  and  $l/h = 20$ ). The response is calculated by the 2D model of the soil layer with finite length and thickness (Fig. 3b). It can be observed that not only the value of the first natural frequency is different (as it is shown in Fig. 20), but there is also significant difference in the. Obviously, the phase angle is also different; when the  $l/h$  ratio is small, the phase angle around the first natural frequency is closer to zero, which means that the damping is much smaller.

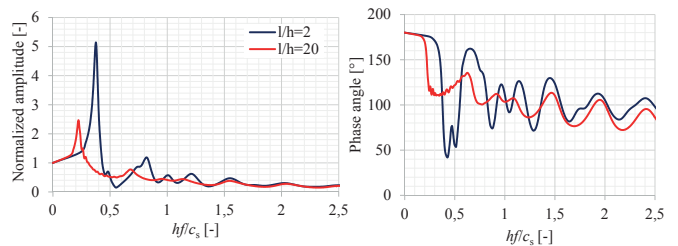


**Fig. 21** Impedance of soil layer with finite thickness ( $h$ ) and length ( $l$ )

## 7.2 Time-history analysis for earthquake-record

In this section the effect of the resonance of a soil layer with finite thickness and length subjected to a real earthquake record is analyzed by direct method. The dominant frequency of the chosen record (Fig. 22) is 0.7 1/s, the first natural frequency of a soil layer with  $h = 50\text{ m}$  and  $l = 150\text{ m}$  is close to this value. Fig. 22 shows that the maximum horizontal displacement of the rigid structure is 1.5 times bigger in this case than the cases when  $l = 100$ , or  $l = 1000\text{ m}$ .

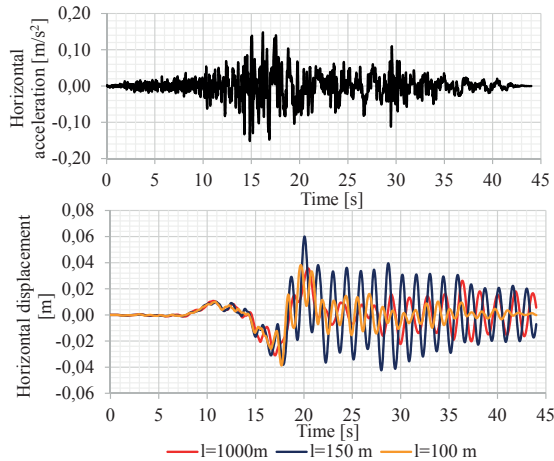


**Fig. 22** Earthquake record (number 21 of the far-field records of [20]) and the horizontal displacement of a rigid structure due to the record ( $h = 50\text{ m}$ ,  $c_s = 100\text{ m/s}$ ,  $\nu = 0$ ,  $\rho = 1800\text{ kg/m}^3$ ,  $\zeta = 0.05$ ,  $r_0 = 10\text{ m}$ ,  $M = 100\text{ t}$ )

## 8 Conclusions

In this paper we investigated the possible errors due to the different modelling of soil structure interaction. Some of the applied soil models, which are extensively used in practical design, the soil substructure has no eigenfrequency, which may lead to significant error and to a not conservative design. For harmonic excitation the error of using the simplified model can be an order of magnitude (Fig. 16), and for earthquakes, where the eigenfrequency of the soil-structure system is close to the dominant frequency of the earthquakes, the predicted maximum displacement of the simplified model can be 10 times smaller than that calculated with the more sophisticated models. Furthermore the effect of the finite length of the layer can also enhance the motion Fig. 22.

The numerical analyses showed that two cases have to be investigated to determine the effect of resonance, the natural frequency of the soil layer and the natural frequency of the soil layer – structure system. The effect of the resonance in case of the soil layer are shown in Fig. 10 and Fig. 14. The difference between the impedances of the soil layer (Fig. 3a) and the simplified model (Fig. 3c) occurs at the first natural frequency. For big  $r_0/h$  ratios the error is more significant than for small  $r_0/h$  ratios.

The first eigenfrequency of the system (soil layer and the foundation with the weight of the rigid structure), can also result in resonance. Fig. 17 shows that the horizontal displacement of the soil-structure model (Fig. 15a) can be 10 times

bigger than the horizontal displacement of the simplified model (Fig. 15b). This significant error occurs in that case, when the first natural frequency of the soil layer is close to the dominant frequency of the earthquake. Fig. 18 shows the parameter range of  $h$  and  $c_s$ , where these two frequencies collide.

## Acknowledgement

This work is being supported by the Hungarian Scientific Research Fund (OTKA, no. 115673).

## References

- [1] Lai, C. G., Martinelli, M. "Soil-Structure Interaction Under Earthquake Loading: Theoretical Framework". *ALERT Doctoral School Soil-Structure Interaction*, (October), pp. 3–43. 2013. [http://alertgeomaterials.eu/data/school/2013/2013\\_ALERT\\_schoolbook.pdf](http://alertgeomaterials.eu/data/school/2013/2013_ALERT_schoolbook.pdf)
- [2] Wolf, J. P., Deeks, A. J. *Foundation vibration analysis: a strength-of-materials approach*. Oxford: Elsevier. 2004. <https://doi.org/10.1016/B978-0-7506-6164-5.X5000-X>
- [3] Kausel, E. "Early history of soil-structure interaction". *Soil Dynamics and Earthquake Engineering*, 30(9), pp. 822–832. 2010. <https://doi.org/10.1016/j.soildyn.2009.11.001>
- [4] Lamb, H. "On the propagation of tremors over the surface of an elastic solid". *Philosophical Transactions of the Royal Society London*, 203(359–371), pp. 1–42. 1904. <https://doi.org/10.1098/rsta.1904.0013>
- [5] Reissner, E. "Stationäre, axialsymmetrische, durch eine schüttelnde Masse erregte Schwingungen eines homogenen elastischen Halbraumes". *Ingenieur-Archiv*, VII(6), pp. 381–396. 1936.
- [6] Sung, T. Y. "Vibration in semi-infinite solid due to periodic surface loadings". *Symposium on Dynamic Testing of Soils, Special Technical Publication*, 156, pp. 35–54. 1954.
- [7] Hsieh, T. K. "Foundation vibrations". *Proceedings of the Institution of Civil Engineers*, 22(2), pp. 211–226. 1962. <https://doi.org/10.1680/iicep.1962.11089>
- [8] Lysmer, J., Richart, F. E. "Dynamic response of footings to vertical loading". *Journal of the Soil Mechanics and Foundations Division*, 92, pp. 65–91. 1966.
- [9] Bycroft, G. N. "Forced Vibrations of a Rigid Circular Plate on a Semi-Infinite Elastic Space and on an Elastic Stratum". *Philosophical Transactions of the Royal Society London*, 248(948), pp. 327–368. 1956. <https://doi.org/10.1098/rsta.1956.0001>
- [10] Shah, P. M. *On the dynamic response of foundation systems*. Rice University. 1968.
- [11] Dobry, B. R., Gazetas, G. "Dynamic response of arbitrarily shaped foundations". *Journal of Geotechnical Engineering*, 112(2), pp. 109–135. 1986. [https://doi.org/10.1061/\(ASCE\)0733-9410\(1986\)112:2\(109\)](https://doi.org/10.1061/(ASCE)0733-9410(1986)112:2(109))
- [12] Mylonakis, G., Nikolaou, S., Gazetas, G. "Footings under seismic loading: Analysis and design issues with emphasis on bridge foundations". *Soil Dynamics and Earthquake Engineering*, 26(9), pp. 824–853. 2006. <https://doi.org/10.1016/j.soildyn.2005.12.005>
- [13] Meek, J. W., Veletsos, A. S. Simple models for foundations in lateral and rockin motion. In: *Proceedings of the Fifth World Conference on Earthquake Engineering*, Rome, 1974. [http://www.iitk.ac.in/nicee/wcee/article/5\\_vol2\\_2610.pdf](http://www.iitk.ac.in/nicee/wcee/article/5_vol2_2610.pdf)
- [14] Barros, F. C. P. D. E., Luco, J. E. "Discrete models for vertical vibrations of surface and embedded foundations". *Earthquake Engineering and Structural Dynamics*, 19(2), pp. 289–303. 1990. <https://doi.org/10.1002/eqe.4290190211>
- [15] Wolf, J. P. "Spring-dashpot-mass models for foundation vibrations". *Earthquake Engineering and Structural Dynamics*, 26(9), pp. 931–949. 1997.

- [16] Hall, J. R. "Coupled rocking and sliding oscillations of rigid circular footings". In: *Proc. Int. Symp. Wave Propag. Dyn. Prop. Earth Matter* (pp. 139–148). Albuquerque, New Mexico: University of New Mexico. 1967.
- [17] Chen, W. F. *Handbook of structural engineering*. Boca Raton, New York: CRC Press. 1997.
- [18] Oskouei, A. G., Oskouei, A. V. "The Effect of P-Wave Propagation on the Seismic Behavior of Steel Pipelines". *Periodica Polytechnica Civil Engineering*, 61(4), pp. 889–903. 2017. <https://doi.org/10.3311/PPci.9866>
- [19] Eurocode. "BS EN 1998-5:2004 - Eurocode 8: Design of structures for earthquake resistance - Part 5: Foundations, retaining structures and geotechnical aspects". 2004.
- [20] FEMAP695. "Quantification of Building Seismic Performance Factors". *FEMA P695*. 2009. [https://www.fema.gov/media-library-data/20130726-1716-25045-9655/fema\\_p695.pdf](https://www.fema.gov/media-library-data/20130726-1716-25045-9655/fema_p695.pdf)